High Resolution Surface-Wave Dispersion Studies in China

Laura E. Jones and Howard J. Patton

High Resolution Surface–Wave Dispersion Studies in China

Laura E. Jones and Howard J. Patton[1]
Los Alamos National Laboratory, Geophysics EES-3, MS-C335, Los Alamos, New Mexico

Abstract

The Los Alamos National Laboratory regional calibration project is actively assembling a database of surface–wave dispersion information for China and surrounding areas. As part of the effort to characterize surface wave dispersion in China, we integrate prior long period results from the University of Colorado with our shorter period dispersion measurements in a high resolution survey of key monitoring areas. Focusing on western China initially, we employ broadband data recorded on CDSN stations, and regional events (m_b 4 and above). Our approach is twofold, employing *path specific calibration* of key stations and well-recorded reference events, and *tomographic inference* to provide group velocity curves for regions with sparse station distribution and little seismic activity. Initial dispersion studies at Chinese stations WMQ and LZH show substantial azimuthal variation in dispersion, reinforcing the need for careful determination of source regions for path-specific calibration.

Key Words: regional seismic characterization, path effects, China, surface waves, tomography

---

Objective of Study

We build on prior work done at the University of Colorado, Boulder (JSPC) by Ritzwoller and Levshin [1997] and Ritzwoller *et al.* [1997]. The present study seeks to integrate longer period results from teleseismic data with results from broadband records recorded at regional distances at stations in China and Eurasia. This smaller scale, higher resolution study focuses on western China initially, employing shorter paths, higher frequency data, and events from China and surrounding regions. Our initial objectives are twofold and include:

1. Path specific calibration: We estimate surface–wave dispersion for key stations and source regions, using well-known (CMT) and well-recorded reference events.

   Such calibration will result in filters designed to extract surface waves in an automated fashion for use in surface wave detection, M_s estimation, discriminants and further structural or attenuation studies.

2. Tomographic inference: We combine our measurements with long period measurements from the University of Colorado for surface–wave tomography.

   We'll use the tomographic results to infer group velocity curves for regions with sparse events and/or station coverage. We then test how effectively the inferred dispersion curves extract surface waves for the purposes outlined above in item 1.

Research Accomplished

Introduction. Regional surface waves carry valuable information for use in the detection, location, and identification of small seismic sources. In principal, techniques for locating and identifying sources developed for teleseismic surface-wave applications might easily be extended to regional problems. One example of high interest is the regional extension of M_s:m_b, one of the most powerful teleseismic discriminants. However, major challenges confront the effective implementation of long-period to short-period discriminants as source size decreases: observations must be made at progressively shorter ranges and degrading signal-to-noise conditions for the long period energy.

With these issues in mind, detection of surface waves is presently an important research topic in CTBT monitoring. Emphasis on small magnitudes and regional observations motivates investigation on the effective extraction of Rayleigh- and Love-wave signals from complex regional waveforms, where phases have not significantly dispersed, where there is potentially significant overlap (in frequency and time) between higher-mode surface-waves and lower frequency body-wave arrivals, and where there may be high levels of ambient background noise.

Regional calibration of key monitoring areas provides information necessary to assess capabilities at small magnitudes and to determine propagation characteristics for signal extraction.

We employ two strategies for building a knowledge base of information for use in extracting fundamental-mode energy from regional waveforms. Both strategies are based on empiricism and both involve designing a match filter with some knowledge of the true surface-wave dispersion on a source-receiver path of interest.

The *path specific* approach uses historic events and waveforms to develop dispersion curves from specific source regions. The second strategy, a *tomographic inference* approach, uses historic data from inside and outside the monitoring region to measure dispersion on many criss-crossing paths, and subsequently images the spatial variations of surface-wave velocities for the key areas.

To some extent these approaches are complementary. While the former will supply highly accurate information for active source regions, the latter will provide adequate information for surface-wave extraction when an unknown source occurs in a new source region. We expand on these issues and our approach below.

Data Collection. We have assembled and continue to process broadband waveform data from IRIS and CDSN stations within and around China. Of special interest to us are the short-path (3° to 15°) surface wave data compiled for western China. Further details and a table summarizing the data are found in this volume (Phillips *et al., 1997*).

Software. We have ported the Ritzwoller and Levshin *Frequency-time analysis* (FTAN) code to our machines, to further ensure the compatibility and smooth integration of our short-path broadband results with existing longer path results from University of Colorado. In addition, this code has the attractive feature that it allows easy selection of the appropriate surface wave mode branch for analysis, helping to separate out fundamental modes on our shorter paths. This processing scheme also allows simultaneous determination of spectral amplitudes and phase and group dispersion.

Preliminary Regionalization Results. Preliminary results are presented in this paper for paths involving two stations of the Chinese Digital Seismic network (CDSN), WMQ and LZH, and events shown as circles or diamonds for earthquakes, and a star for East Kazakh explosions [Figure 1].

One pressing issue in our study concerns the detection of surface waves as a function of magnitude and distance. In areas of the western United States, regional surface waves with periods between 8 - 50 sec are recorded well enough to be used in moment tensor inversions of earthquakes as small as m_b 3.5 (Patton and Zandt, 1991; Romanowicz et al., 1993). Despite the relative complexity of structures in western China, surface waves appear to be cleanly recorded on some far-regional paths to small magnitudes. To illustrate this, we show a Rayleigh-wave record section using the events plotted as diamonds on Figure 1 [Figure 2, right-hand panel]. Broadband records have been filtered to enhance the surface waves. These results show that events with m_b in the mid-4 range are well recorded across the Tibetan Plateau out to at least 1500 km. The record section also shows the evolution of wave-trains with distance, illustrating compact waveforms at short distances and better-separated, more easily identifiable fundamental-mode surface waves at far distances.

Definition of distinct source regions for the *path specific* approach is a major consideration in our work. This is driven by the scale of heterogeneity the extent to which dispersion curves vary laterally. We illustrate this on the left-hand side of Figure 2 with waveform data from LZH. Again, broadband data have been filtered to show the surface-wave arrivals for five events in source region **A**, a compact source site about 25 km across. At a distance of about 800 m, we find that surface waves are well–recorded for the m_b range 4.1 - 6.2. All waveforms display very similar "inverse" dispersion characteristics for the 15 - 40 sec period

range visible after filtering. Waveforms are presented for two other source regions at about the same range as **A**, but different backazimuths. The dispersion characteristics for these events may be different enough to define two more source regions distinct from region **A**. Tests need to be devised to evaluate criteria for source region definition.

Similarly, preliminary dispersion results for station WMQ underscore the need for path-specific calibration, and also for limiting the size of a specific source area in path calibration. We have collected and processed three-component broadband date for 26 CMT events recorded at station WMQ. Group velocities for Love and Rayleigh waves were measured at periods of 10 to 50 seconds. Resulting dispersion curves for paths around WMQ are generally consistent with a modified Eastern Tien Shan earth model (Figure 3ab, bold curve) but nonetheless show significant azimuthal variation. Curves for paths through the Jungarrian basin (fine dashed line; Figure 1, Figure 3) show the effects of slow basin structure at higher frequencies. Note that prior long–period studies do not resolve the Jungarrian basin, but our higher resolution work clearly will.

Recommendations for Future Work

Along with the ongoing measurement of dispersion curves for specific source sites and stations, we'll devise tests to determine the lateral extent of such source regions to increase the reliability and robustness of our *path specific* approach. Dispersion curves inferred from our tomographic maps will be tested for their effectiveness in signal extraction, and the maps may be modified accordingly. We plan analysis of spectral amplitudes and the eventual construction of an attenuation map for western China and later, Asia. Finally, the accumulated broadband data allows the possible use of body waves and higher modes for source parameter studies, including accurate determination of depth.

References

Patton, H. J., and G. Zandt, Seismic Moment Tensors of Western U. S. Earthquakes and Implications for the Tectonic Stress Field, *J. Geophys. Res.*, Vol. 86, B11, 18245-18259, 1991.

Phillips, W. S., G. E. Randall, H. E. Hartse, S. R. Taylor and H. J. Patton, Source and Path Effects on Regional Phases in China, *19th Ann. Seismic Research Symp. on Monitoring a Comprehensive Test Ban Treaty*, (this volume), 1997.

Ritzwoller, M. H., and A. L. Levshin, Eurasian Surface Wave Tomography: Group Velocities, *J. Geophys. Res.*, submitted, March 1997.

Ritzwoller, M. H., A. L. Levshin, L. I. Ratnikova, and A. A. Egorkin, Intermediate Period Group Velocity Maps Across Central Asia, Western China, and Parts of the Middle East, *J. Geophys. Res.*, submitted, May 1997.

Romanowicz, B., D. Dreger, M. Pasyanos and R. Uhrhammer, Monitoring of Strain Release in Central and Northern California Using Broadband Data, *Geophys. Res. Lett.*, Vol. 20, No. 15, 1643-1646, 1993.
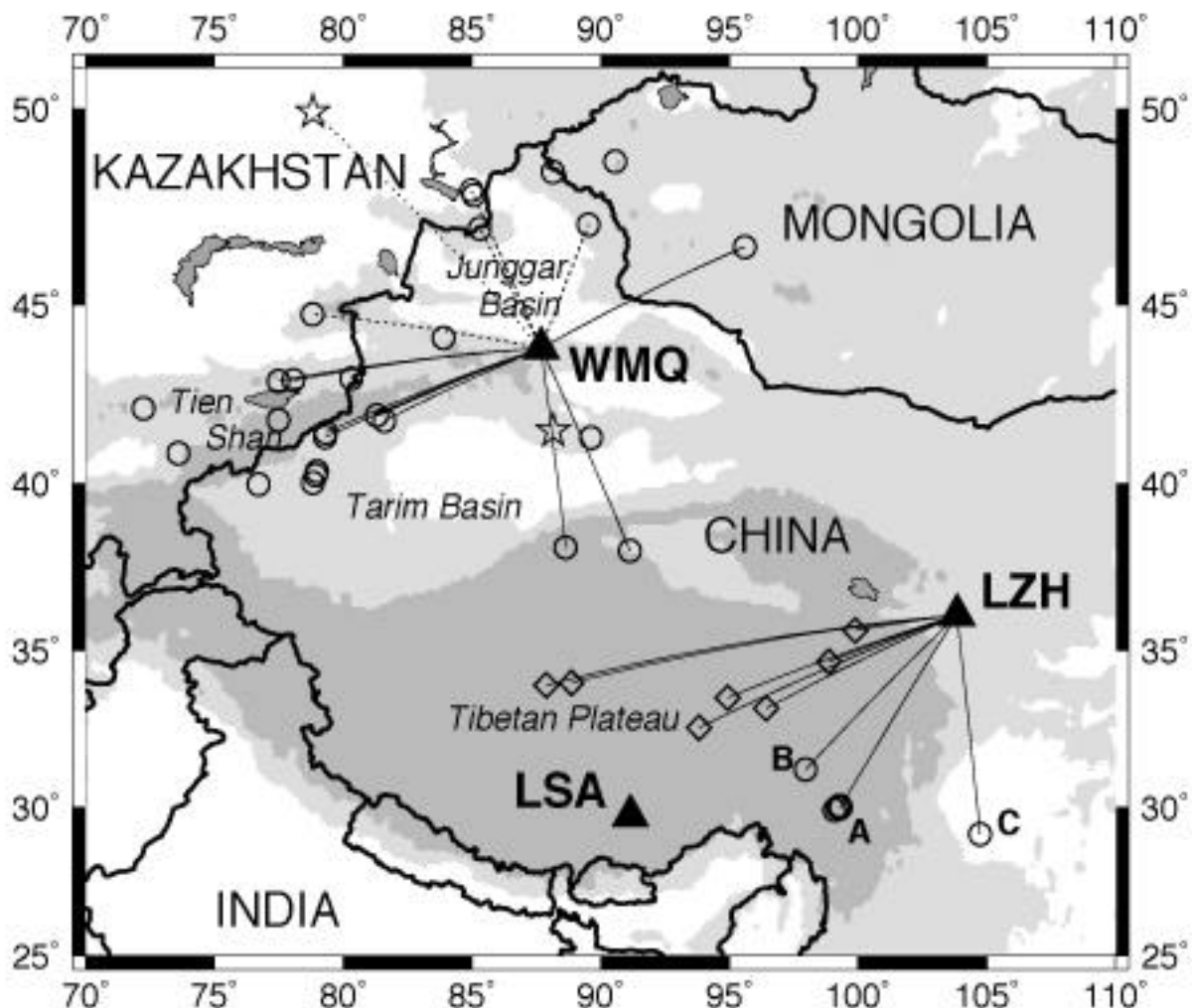
Figure 1. Map of study area showing locations of stations, events, and paths discussed in this paper. Elevations are shown as shades of grey in three intervals: -100 to 1000 m above sea level, no shading; 1000 to 3000 m, light grey; and above 3000 m, darker grey. Large bodies of water are shown by the darkest grey areas. Source regions **A**, **B**, and **C**, discussed in the text, are identified on the map. Earthquakes used in making the Rayleigh-wave profile in Fig. 2 are plotted as diamonds. Other earthquakes are plotted as open circles, and the East Kazakh and Lop Nor test sites as open stars. Great circle paths are shown as lines. Dotted lines are those paths through the Junggarrian Basin with slow group velocities at short periods in Fig. 3ab.

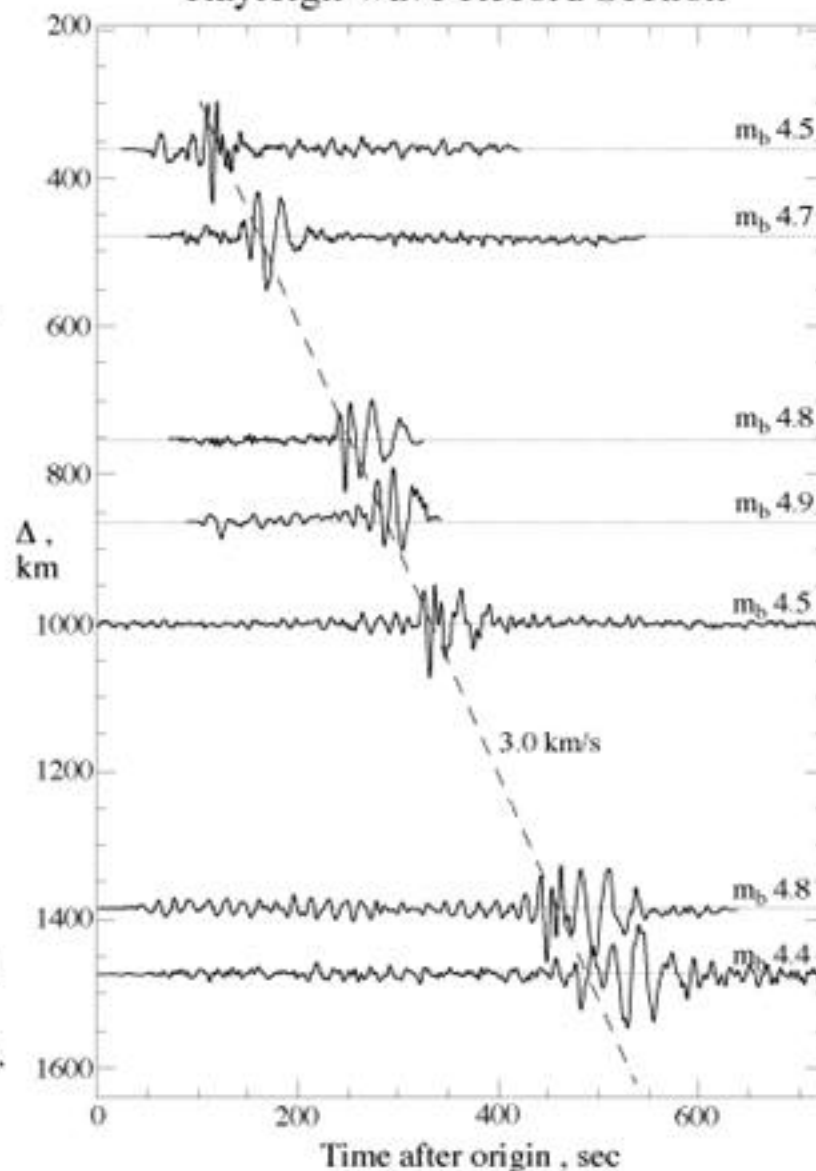# Rayleigh waves, LZH
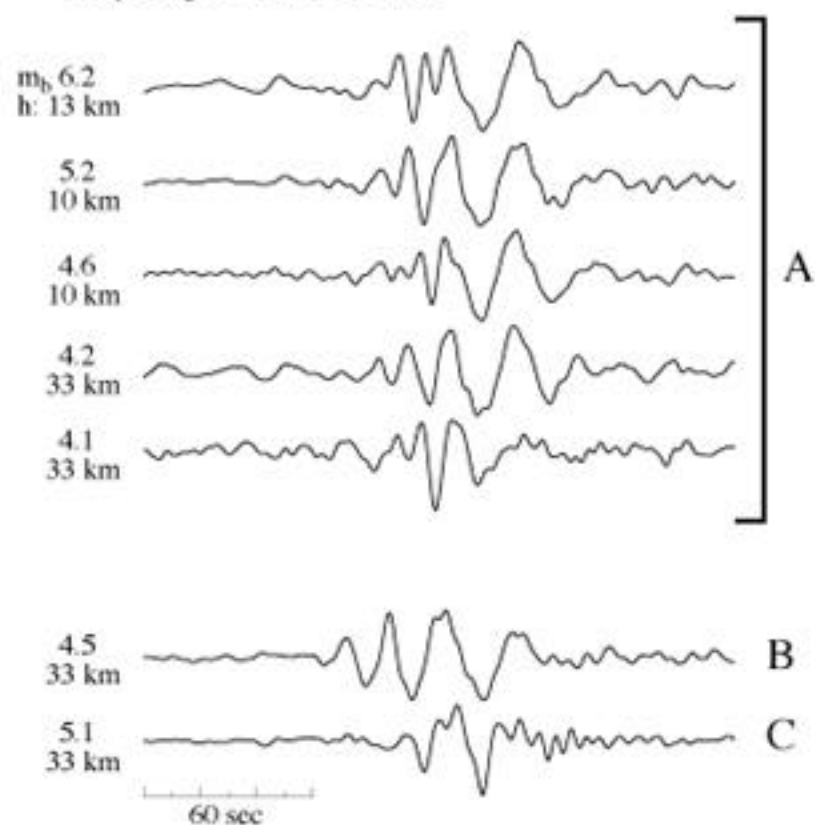
Rayleigh-wave Record Section

Figure 2. Vertical component recordings at station LZH low-pass filtered at 0.03 Hz. The traces on the left have been phase equalized by simply time aligning on the largest downswing. Three source regions are shown: **A** at an average distance of 803 km and back-azimuth of 214°; **B** 767 km, 227°; and **C** 779 km, 174°. On the right, a record section is plotted for earthquakes located on the Tibetan Plateau for backazimuths between 246° and 265°. See the map in Figure 1 for reference.
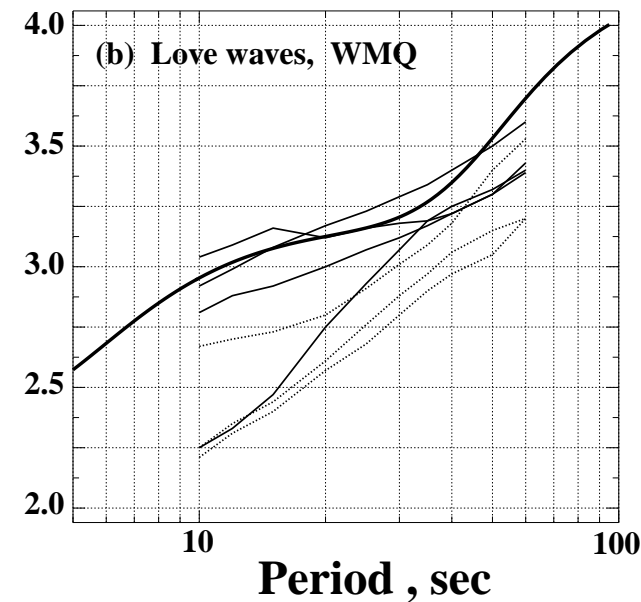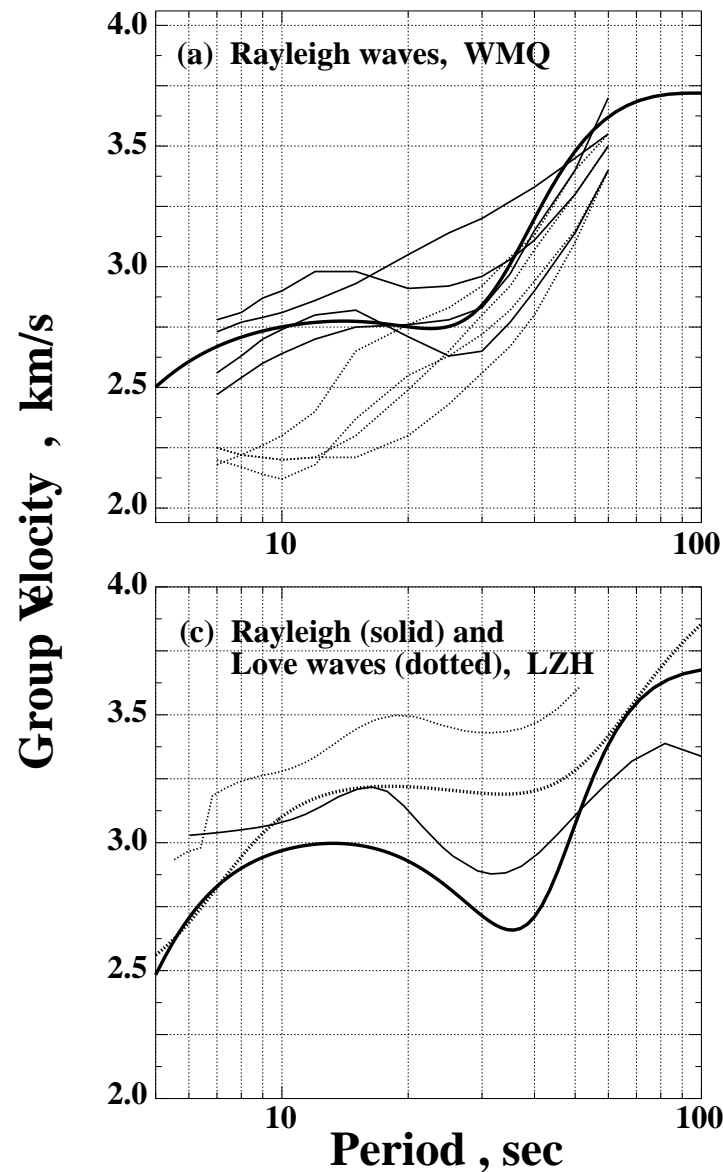
Figure 3. Group velocity dispersion curves for selected paths in western China. (a) Rayleigh-wave dispersion curves are broken down into two groups: paths that pass through the Junggarian Basin (dotted) and those paths that sample mainly crystalline basement paths (solid). See Figure 1. (b) Same as (b) but for Love waves. In both (a) and (b), a model group velocity curve is shown, which is based on a modified crustal structure from Ksarev et al., (1993; JGR,98, p.4437) with a PREM upper mantle. (c) Thin lines are observed dispersion curves between source region A and LZH on the Tibetan Plateau. For comparison, we show model dispersion curves predicted by crustal model 45 of Romanowicz (1982; JGR,87, p.6865) with a PREM upper mantle. Model dispersion curves generally agree in shape with the observed, but some significant differences exist probably due to lateral heterogeneity